Maintaining forest cover to enhance temperature buffering under future climate change

Global Ecology and Biogeography

A
Mac

Maintaining forest cover to enhance temperature buffering under future climate change

Journal:	*Global Ecology and Biogeography*
Manuscript ID	GEB-2021-0524
Manuscript Type:	Research Article
Keywords:	forest microclimate, temperature offsets, canopy, climate change, future climate projections, forest biodiversity, macroclimate, paired sensor data

Maintaining forest cover to enhance temperature buffering under future climate change

Abstract

Aim: Forest canopies buffer macroclimatic temperature fluctuations. However, we do not know how much forest understorey temperatures will change with accelerating climate change. Here, we aimed at mapping the difference (offset) between temperatures inside and outside forests in the recent past and in the future in boreal, temperate and tropical forests.

Location: Global.

Time period: Predictions for past (1970-2000) and future (2060-2080) conditions.

Major taxa studied: Trees and shrubs.

Methods: Using linear mixed-effect models, we combine a global database of 714 paired time series of temperatures (mean, minimum and maximum) measured inside forests vs. in open habitats with maps of macroclimate, topography and forest cover to hindcast past (1970-2000) and to forecast future (2060-2080) temperature differences between free-air temperatures and sub-canopy microclimates.

Results: For all tested future climate scenarios, we predicted that offsets for maximum temperature in forests across the globe will become, on average during 2060-2080, more negative due to changes in macroclimate temperature and precipitation. This suggests that extremely hot temperatures under forests canopy will, on average, rise slightly less than outside forests as macroclimate warms.

Main conclusion: This knowledge is of utmost importance as it suggests that forest microclimates will warm at a slower rate than non-forested areas, assuming that forest cover is maintained. This highlights the potential role of forests as a whole as microrefugia for biodiversity under future climate change.

Introduction

Warming temperatures and changing precipitation regimes are influencing ecosystems across the globe (IPCC, 2018). To date, ecological research assessing the impact of anthropogenic climate change has predominantly relied on macroclimatic data. These data are typically based on a global network of weather stations established at approximately 1.5 to 2.0 m above the soil surface in open habitats (e.g. above short grass) (World Meteorological Organization, 2018). Forest organisms living below and within tree canopies, however, experience microclimatic conditions distinct from those in open habitats (J. Chen et al., 1999; De Frenne et al., 2021; Geiger, Aron, & Todhunter, 2009). Below tree canopies, lower radiation, wind and evapotranspiration rates often translate into lower temporal variation in air temperature and humidity compared to open environments (Davis, Dobrowski, Holden, Higuera, & Abatzoglou, 2019; Geiger et al., 2009; Von Arx, Graf Pannatier, Thimonier, & Rebetez, 2013). In particular, temperature extremes are often strongly attenuated in forest interiors, with lower maxima and higher minima compared to open environments (De Frenne et al., 2019; Li et al., 2015). Studies have already shown that such microclimatic buffering can mediate the response of forest communities to climate change (De Frenne et al., 2013; Dietz et al., 2020; Lenoir, Hattab, & Pierre, 2017; Stevens, Safford, Harrison, & Latimer, 2015; Zellweger, De Frenne, Lenoir, Vangansbeke, Verheyen, Bernhardt-Römermann, et al., 2020). Despite the increasing evidence that ecosystem dynamics and processes are more likely to be related to forest microclimates than to macroclimate (Y. Chen et al., 2018; De Frenne et al., 2021; De Smedt, Boeraeve, & Baeten, 2021; Frey, Hadley, & Betts, 2016), microclimates are still seldom incorporated in ecological research (e.g. in species distribution models) (Lembrechts, Nijs, & Lenoir, 2019) and ignored by dynamic global vegetation models (DGVMs; e.g. Thrippleton, Bugmann, Kramer-Priewasser, & Snell, 2016) that simulate the effects of future climate change on natural vegetation and its carbon and water cycles. In particular, we do not know how forest microclimates will change in the future as macroclimate changes (Lembrechts & Nijs, 2020).

Advances in studies on the effects of climate change on different organisms living below or in forest canopies have often been limited by the availability of suitable microclimatic data (De Frenne et al., 2021). One robust way to study forest microclimates is to use microclimate measurements from paired (inside *vs.* outside

forests) sensor networks to calculate temperature offsets, i.e. the absolute and instantaneous difference between temperature inside (i.e., microclimate) and free-air temperatures outside forests (i.e., macroclimate) (*sensu* De Frenne et al., 2021). Negative offset values thus reflect cooler and positive offsets warmer forest temperatures compared to outside forests. These empirical offset values for temperature can be related to readily available environmental data using statistical modelling approaches, and these models can then be used to interpolate and extrapolate microclimate across entire mapped landscapes (Frey, Hadley, Johnson, et al., 2016; Greiser, Meineri, Luoto, Ehrlén, & Hylander, 2018). Differences between macro- and microclimate (i.e., temperature offsets) result from processes operating at many scales that influence incoming solar radiation, air mixing, soil properties or evapotranspiration (reviewed in De Frenne et al., 2021). Macroclimatic conditions (e.g., mean temperature and rainfall), topographic variation in the landscape (e.g., elevation and aspect) and variation in canopy cover and vegetation height have been reported to be the main drivers of the understorey temperatures in forests (De Frenne et al., 2021, 2019; Greiser et al., 2018; Macek, Kopecký, & Wild, 2019; Zellweger et al., 2019). With the advent of global forest microclimate data (De Frenne et al., 2019; Zellweger, De Frenne, Lenoir, Vangansbeke, Verheyen, Bernhardt-Römermann, et al., 2020), this type of modelling now enables the prediction of forest microclimates across forest types under future climate change.

Here, we attempt to map recent past and future forest microclimate temperature offsets using statistical models based on paired sensor measurements (below-canopy vs. open-air temperature at a given site) and landscape- and canopy-scale predictors (Fig. 1; Supplementary Fig. 1). Predictions were made for mean, minimum and maximum temperatures (further referred to as T_{mean}, T_{min} and T_{max}, respectively) throughout the year for the Earth's dominant forested ecosystems (boreal, temperate and tropical forests) across five continents. We made predictions of the temperature offsets using macroclimatic data for past (1970-2000) and future (2060-2080) climatologies. To predict these offsets, we used linear mixed-effect models to test their response to macroclimatic conditions (e.g. mean temperature and rainfall), topographic variation in the landscape (e.g. elevation and aspect) and variation in canopy cover and vegetation height at a global extent and at a spatial resolution of 30 arcsec (~1 km at the equator, see data references).

Material & Methods

Paired plot data

We used a unique data set with 714 temperature offset data points involving paired plots from 74 studies spread across 5 continents (Supplementary Fig. 1; Data available in De Frenne et al., 2019). A key asset of this database is the paired nature of the data, which always combines below-canopy temperature data at a given forest site with open-air temperature data from a neighbouring non-forest site using a similar design (same logger and shielding material installed at the same height between open and forest conditions). We specifically refrained from using additional data on forest microclimate conditions that were not strictly paired with free-air conditions from a neighbouring site using the exact same design (same sensor, same logger, same shielding material, same height). The data points were collated from the scientific literature in a systematic and reproducible manner (see De Frenne et al., 2019 for full details). Temperature offsets were calculated as the temperature inside the forest minus the temperature outside the forest, or extracted directly from the original study; negative values reflect cooler temperatures below tree canopies while positive values reflect warmer understorey temperatures. This was done for three temperature response variables, i.e. mean (T_{mean}), maximum (T_{max}), and minimum (T_{min}) temperature that were computed during a specific time period that could differ between sites but that was exactly the same between paired sensors installed outside and inside the forest at a given site. Multiple forest sites (at least several kilometres apart), seasons (meteorological seasons, later aggregated to growing versus non-growing season) and temperature metrics (maximum, mean, minimum, air or soil temperatures) originating from the same study were entered into different rows of the database but tagged under the same study ID. Temperature values of long time series were always aggregated per season and/or year, which means that several temperature values for T_{mean}, T_{min} or T_{max} could be generated for the same study site. Temperature measurements were classified as having taken place during the growing season, the non-growing season or throughout the whole year. This classification was performed on the basis of reported meteorological seasons and/or climate information in the original study. The dry and winter season were classified as the non-growing season in tropical and temperate biomes, respectively. Estimates of uncertainty (standard error, standard deviation, coefficient of

variation or confidence intervals) of the temperature measurements were only reported for a small minority (13.6%) of offset values in the database and were thus not included in our analyses. See De Frenne et al. (2019) for more details on the literature search, inclusion criteria and the empirical data used in this study.

Predictor variables

To predict the offsets for the three temperature variables (T_{mean}, T_{max}, T_{min}) across all forests at a global extent, we gathered global maps of predictor variables related to macroclimate, topography and forest cover. These three sets of predictor variables were selected based on their importance for forest microclimate, and on the spatial resolution and extent of the available data. All the predictor maps we used are raster maps with a spatial resolution of 30 arcsec (~1 km) and are available at the global extent (i.e., from 80°N to 56°S in latitude and from 180°E to 180°W in longitude). Values for all predictor variables were extracted using the geographical coordinates for each plot pair.

Macroclimate. Global raster maps of mean, minimum and maximum free-air temperature (°C; T_{macro}), on a monthly basis, as well as monthly precipitation (mm) raster maps, averaged for the climatology 1970-2000, were collected from WorldClim version 2.1 (Fick & Hijmans, 2017). In addition, we gathered future projections (2060-2080) for the exact same set of temperature and precipitation variables described in the previous sentence but based on the contrasting "very stringent" representative concentration pathway (RCP) 2.6 and "worst case" RCP 8.5 from three different general circulation models (GCMs) with minimal interdependency, based on Sanderson, Knutti and Caldwell (2015), i.e. HadGEM2-ES, MPI-ESM-LR and MIROC5 (downscaled CMIP5 data from WorldClim; 30 arcsec resolution).

Topographic variables and distance to the coast. We gathered six variables related to topography using raster layers derived from the Global Multi-resolution Terrain Elevation Data 2010 (GMTED2010) dataset at 30 arcsec resolution (Amatulli et al., 2018). Maps on northness and eastness, elevation (m a.s.l.), elevational variation (EleVar) and topographic position index (TPI) were collected. Northness and eastness are the sine of the slope, multiplied by the cosine and sine of the aspect, respectively. They provide continuous measures describing the orientation in combination

with the slope (i.e., a circular variable is transformed into a continuous one, ranging from -1 to 1). In the Northern Hemisphere, a northness value close to 1 corresponds to a northern exposition on a vertical slope (i.e., a slope exposed to very low amount of solar radiation), while a value close to -1 corresponds to a very steep southern slope, exposed to a high amount of solar radiation. Aspect values for the Southern Hemisphere were inverted so that a value of 1 in the Southern Hemisphere also means very low amount of solar radiation. Variables EleVar (1) and TPI (2) capture topographic heterogeneity within a 1 km² grid cell around each pair of measurements (inside and outside forest): (1) the standard deviation of elevational values aggregated per 1 km² grid cell (further referred to as elevational variation) and (2) the median of the topographic position index (TPI) values across each 1 km² grid cell. The TPI is the difference between the elevation of a focal cell and the mean elevation of its eight surrounding cells. Positive and negative values correspond to ridges and valleys, respectively, while zero values correspond to flat areas (Amatulli et al., 2018). We also produced a map with the distance from each land pixel to the nearest coastline (Dist2Coast) using the coastline map data from Natural Earth (free vector data from naturalearthdata.com).

Forest cover and forest height. We used the tree canopy cover (defined as canopy closure for all vegetation taller than 5 m in height) map for the year 2000 by Hansen et al. (2013). This high-resolution global map layer was re-projected and aggregated from 30 m to 30 arcsec using the average of the aggregated raster cells. This canopy cover map is the only available map spanning a global extent at this high resolution. By using this data product, we make the strong assumption that canopy cover at the time of temperature measurements is similar to the cover in the year 2000. We consider this assumption as reasonable as the median year of the temperature measurements for all data points is approximately 1996 (range between 1943 and 2014). Finally, we used estimates of canopy height at 1 km resolution derived from the ICESat satellite mission based on 2005 (Simard, Pinto, Fisher, & Baccini, 2011).

Data analysis

All statistical analyses were performed in the open-source statistical software environment of R, version 4.0.2 (R Core Team, 2021). The temperature offsets for T_{mean}, T_{max} and T_{min} were modelled (274, 184 and 202 plot pairs respectively), after removing missing values for sensor height, i.e. not mentioned in the original study, and data points with canopy cover zero (based on the tree canopy cover map introduced above; Hansen et al., 2013) using linear mixed-effect models with random intercept (LMMs) (*lme4* package; Bates, Maechler, Bolker, & Walker, 2015). In our main models, we combined the seasonal (growing vs. non-growing and annual) time series and performed additional analyses for the different three different time periods (see further and supporting data Appendix 1). We included 'study ID' as a random intercept term to account for non-independence between samples within studies. For each of the three studied response variables, we started our modelling protocol from the full model:

T_{offset} ~ T_{macro} + Precipitation + Elevation + Eastness + Northness + EleVar + TPI + Dist2Coast + Canopy cover + Forest height + Sensor height + *random effect 'study ID'*

For T_{macro}, we used the monthly average for either T_{mean}, T_{max} and T_{min} temperature during the period 1970-2000 depending on the studied response variable of T offset (T_{mean}, T_{max} or T_{min}). Sensor height was also included in the models (continuous variable, in metres above or below the soil surface), as this significantly impacts the magnitude of the temperature offset (De Frenne et al., 2019; Supplementary Fig. 2). Sensor height is positive for aboveground and negative for belowground sensors. Data points with sensor height > 2 m were excluded as our aim was to model forest microclimate near the ground. To avoid collinearity in predictor variables and improve model performance, we excluded variables that showed a correlation $r \geq |0.7|$ (Pearson's product-moment correlation; Supplementary Fig. 3) and variance inflation factor ≥ 4 (Zuur, Ieno, & Elphick, 2010). Forest height was therefore removed from all models due to high correlation with canopy cover; for T_{mean} offset, EleVar was also dropped from the model due to high correlation with TPI. All predictors were standardized by subtracting the mean and dividing by the standard deviation prior to modelling. For each response variable, the single best model was selected based on the Akaike Information Criterion (AIC) using the automated dredge-function of the package MuMIn (Barton, 2009). Goodness of fit was calculated following Nakagawa and Schielzeth (2013).

To test for non-linear relationships, we also used generalized additive mixed-effect models (GAMMs) (cf. the *gamm4* package) (Wood & Scheipl, 2014) on the same dataset. We applied smoothers to the same set of fixed-effect terms, included the same random intercept term 'study ID' and followed the same model selection procedure as for the LMMs. For each of the three studied response variables (T_{mean}, T_{max}, T_{min}) and for each of the two modelling approaches, we performed a leave-one-out cross validation (LOOcv) and compared root mean square errors (RMSE) among models (LMMs vs. GAMMs). We found no difference (t test, p-value > 0.05) in RMSE between LMMs and GAMMs, justifying our choice of LMMs (see also Supplementary Fig. 5). Furthermore, we checked spatial autocorrelation in the model residuals for the LMMs using Moran´s I-test from the *ape* package (Paradis & Schliep, 2019). No spatial autocorrelation was detected (p-value > 0.05) in our models' residuals. Additionally, we tested the effect of season of sampling (annual, growing and non-growing season; see above) on each response variable. We included season as a categorical variable to the full models described above and followed the same model selection procedure. However, due to the low number of observations for each category (but growing season being the dominant category), results including season were only included in the supporting data Appendix 1.

Using the single best LMMs for each of our three response variables, we made predictions for T_{mean}, T_{max}, and T_{min} offsets for forest across the globe using the collected map data for all predictor variables retained in the models, setting sensor height to 1.0 m and not considering variation included in the random intercept. Temperature offsets were predicted for all raster pixels (30 arcsec resolution) with canopy cover >50% as this largely concurs with the global distribution of forest areas in the terrestrial ecoregions map by Olson et al. (2001). To assess model performance, we performed spatially blocked k-fold cross-validation (k = 10; folds assigned randomly, with spatial blocks of size 50 km²; Alavi, Ahmadi, Hosseini, Tabari, & Nouri, 2019). Furthermore, we made predictions of future forest temperature offsets based on the future projections of temperature and precipitation (the latter only included in the best model for T_{mean} and T_{min}) from WorldClim (see above). We made future predictions for the period of 2060-2080 using the RCP 2.6 and RCP 8.5 projections based on the three selected GCMs to account for uncertainty related to the GCMs; final model predictions for each RCP scenario were averaged over all GCMs. For the future predictions, we assumed no change in topography and conservatively assumed no change in canopy cover as our main goal was to

determine direct climate change effects on temperature offsets below forest canopies if we maintain the forest cover. Of course, we could use different scenarios of future forest cover but we decided to not do that to better assess the unique effect of future climate change without changing other parameters, such as forest cover, in the model. Besides, future scenario on forest cover are not yet available at a global extent and at the spatial resolution we used here. Uncertainty in predictions was mapped by applying a bootstrap approach. We resampled the original data used to fit the models with replacement with total size of the bootstrap samples equal to the size of the original sample. For each of the temperature responses, we fitted single best models using 30 bootstrap samples. Using these 30 models, we generated per-pixel standard deviation mapped at the global extent (Supplementary Fig. 8). To map uncertainty for the future predictions, the same procedure was followed for each of the three GCMs, i.e. 30 bootstraps per GCM. Furthermore, we provide maps indicating where the models are extrapolating beyond the values of data used to fit the models. Predictive performance and uncertainty mapping were performed considering fixed effects of the models, excluding uncertainty of the random (study) effects. Predictions were made using the *raster* package (Hijmans & van Etten, 2012). Graphical plots were created using *ggplot2* (Wickham, 2016) and *Tmap* packages (Tennekes, 2018).

Results

Our models predicted an average global offset of -2.92 ± 1.57 °C (mean ± SD) for T_{max}, -0.88 ± 1.82 °C for T_{mean}, and 0.96 ± 1.27 °C for T_{min} (Fig. 1 and 2). These averages were calculated from all pixels having at least 50% canopy cover during the year 2000 (Hansen et al., 2013) and derived from the predictions in Fig. 1 and Supplementary Fig. 4. Our predictions show a slightly positive T_{mean} offset (i.e. warmer temperatures within the forest) in boreal forests, becoming overall negative towards the tropics (i.e. cooler temperatures within tropical forests compared to free-air temperatures) (left panels Fig. 2). T_{max} offsets are negative across the three biomes (i.e. cooler maximum temperatures within forests) with the lowest values in the tropics (up to 5 degrees cooler within forests), whereas T_{min} offsets are positive in boreal and temperate forests and negative in the tropics (Fig. 2). When including season in the modelling procedure, we found that for T_{mean}

offsets were lower during the growing season than for the non-growing season across the three biomes. For T_{max} and T_{min}, season was not included in the best model (more detailed results included in Appendix S1).

Offsets for T_{max}, T_{mean} and T_{min} were negatively affected by free-air, macroclimate temperatures (Supplementary Fig. 2 and Table 1). For T_{mean} and T_{min}, we found lower offset values with higher amounts of precipitation (Supplementary Fig. 2 and Table 1), for T_{mean} this indicates stronger buffering (more negative offsets), whereas for T_{min} this means weaker buffering (offsets closer to zero). We found T_{min} offsets to be more positive, i.e. more strongly buffered, in areas with higher canopy cover, on pole-facing slopes and closer to the coast. The marginal R^2 values (for fixed effects) were 0.29 (0.03 SD), 0.21 (0.03 SD) and 0.25 (0.03 SD), while conditional R^2 values (for fixed and random effects) reached 0.58 (0.04 SD), 0.60 (0.06 SD) and 0.52 (0.04 SD) for T_{max}, T_{mean} and T_{min}, respectively. Root mean square errors obtained from the spatial cross-validation were 3.67 °C (1.55 SD), 1.78 °C (0.71 SD) and 1.52 °C (0.45 SD) for T_{max}, T_{mean} and T_{min}, respectively. Standard deviations obtained from the bootstrapping procedure show fair consistency between the predictions of the 30 bootstrapped models (Supplementary Table 2; Supplementary Fig. 6 and 7). Upper confidence levels (95%) of standard deviations for all three responses remained lower that 1 °C (Supplementary Table 2 and Fig. 7). Higher values were mainly observed in the tropical and boreal region. We also found higher extrapolation for the predictors included in the models in tropical forests and especially in the boreal region (Supplementary Fig. 8).

Our future projections showed an overall decrease in offset values for all three temperature responses (Fig. 2; Supplementary Fig. 4). For T_{mean}, future minus past offsets were -0.22 ± 0.16 °C (mean + SD) for RCP2.6 and -0.5 ± 0.22 °C for RCP8.5 (Fig. 2; Supplementary Fig. 4). For T_{max}, future minus past offsets were -0.27 ± 0.16 °C for RCP2.6 and -0.60 ± 0.14 °C for RCP8.5 (i.e. cooler maximum temperatures within forests compared to outside temperatures in the future). For T_{min}, future minus past offsets were -0.12 ± 0.18 °C for RCP2.6 and -0.27 ± 0.24 °C for RCP8.5. These averages were derived from the right panels in Fig. 2 and Supplementary Fig. 4. For both T_{max} and T_{mean}, this means stronger offsets or buffering (more negative offsets), whereas for T_{min} weaker buffering (offsets closer to zero). Decreases in T_{min} offsets are most pronounced in the boreal and temperate region (left panels Fig. 2).

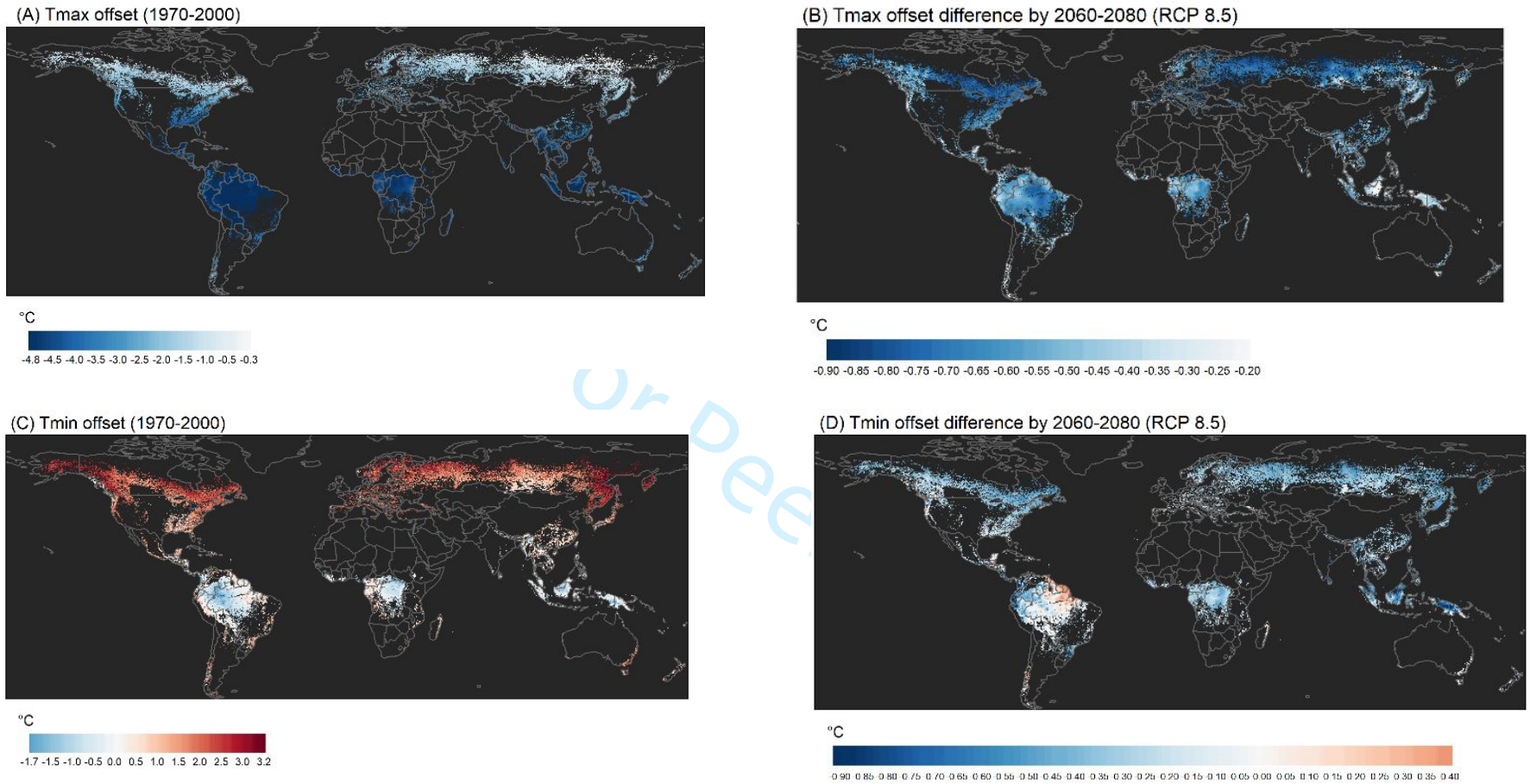

Fig. 1. Left panels: Global maps of past (1970-2000 climate) forest temperature offsets of (A) maximum and (C) minimum temperatures below tree canopies. Right panels: Maps showing the difference between (B) maximum temperature and (D) minimum temperature offset predictions based on future climatic conditions under RCP8.5 scenarios and past (1970-2000) offsets (future minus past, negative values thus depict lower offsets in the future than in the recent past which mean higher buffering for T_{max} but lower for T_{min}). Predictions were made based on linear mixed-effects models and only for pixels where the canopy cover in the year 2000 is > 50% (Hansen et al., 2013). Maps for T_{mean} are shown in supplementary Fig. 4.

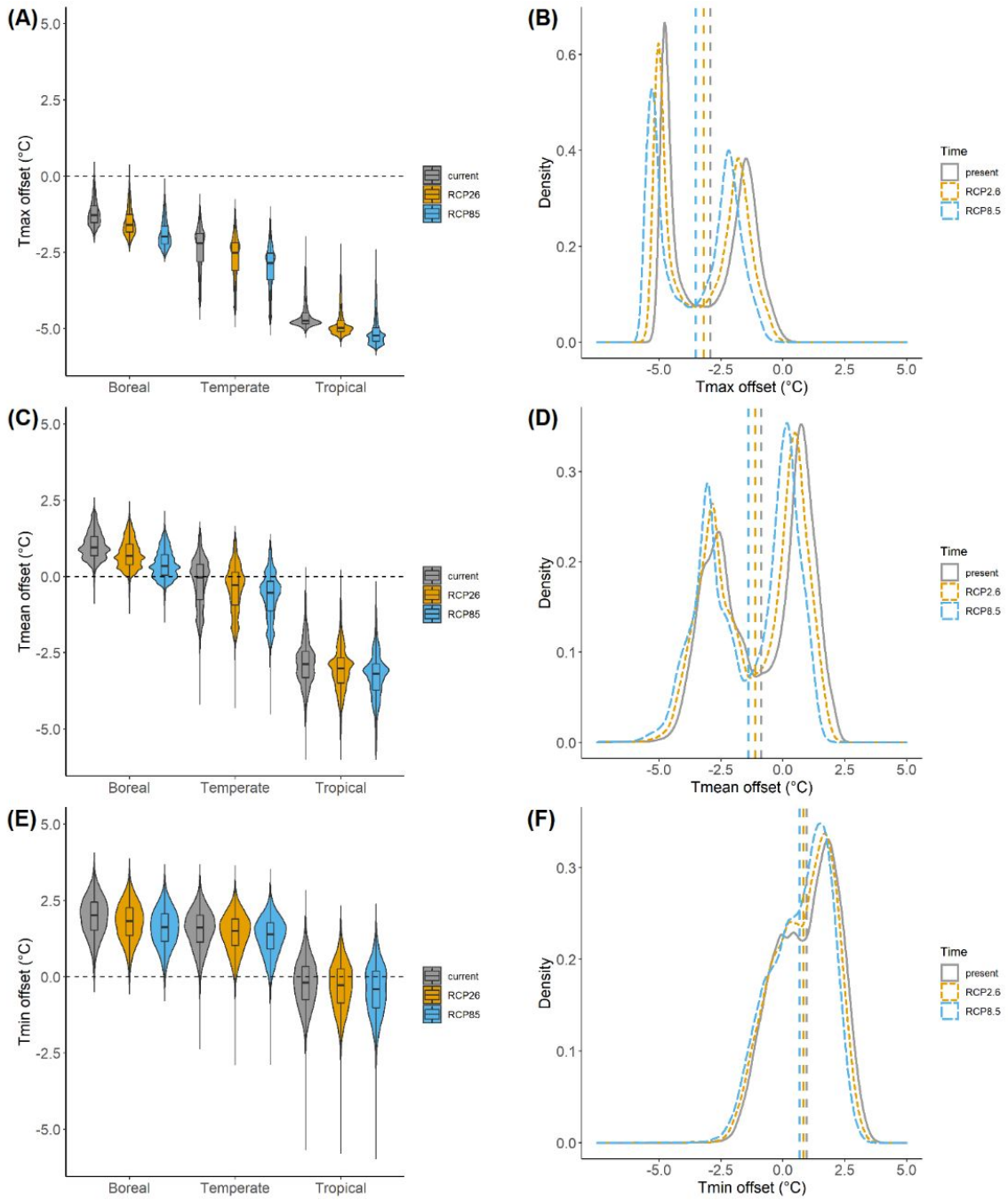

Fig. 2. Left panels: Violin and box plots showing the distribution of predicted below-canopy forest temperature offsets of (A) T_{max}, (C) T_{mean}, and (E) T_{min} across boreal, temperate and tropical forests classified following Olson et al. (2001). Right panels: density plots for the predicted offsets of (B) T_{max}, (D) T_{mean}, and (F) T_{min}. Dashed vertical lines represent global mean offset values for the three temperature responses for past, and the future RCP2.6 and RCP8.5 scenarios. Note that bimodality is observed in the density plots, resulting from the difference between offsets in temperate and boreal versus tropical forests (see Fig. 1). For all plots, different colours and line types represent predictions for past climatic conditions (macroclimate temperature and precipitation, grey), for RCP2.6 (orange) and RCP8.5 scenarios (blue). Data points to draw these plots are subsamples (10^5 pixels) derived from the global predictions in Fig. 1 and Supplementary Fig. 4.

Discussion

Our predictions of temperature offsets for the 1970-2000 climatology and for forests having at least 50% tree cover during the year 2000 (Hansen et al., 2013) show that mean temperatures are on average cooler below canopies (at 1 m height) than in open habitats across all forested grid cells (De Frenne et al., 2019; Li et al., 2015). Our results also support the fact that temperature extremes are mainly buffered in forests; T_{max} is on average lower inside forests, whereas T_{min} is warmer. Nevertheless, strong biome-specific variation was observed: while in boreal forests, T_{mean} offsets were slightly positive, they became overall negative towards the tropics. T_{max} offsets were negative across the three biomes with the most negative values in the (warmer) tropics, whereas T_{min} offsets were positive in the cooler boreal and temperate forests, and negative in the warm tropics. Furthermore, the difference between growing and non-growing season on T_{mean} offsets illustrates the importance of considering the temporal and seasonal variation in temperature offsets in future research (Li et al., 2015; Zellweger et al., 2019).

Temperature offsets for all three responses were negatively related to macroclimate temperatures. This relationship is expected as temperature offsets are directly linked to macroclimate temperatures; if free-air temperatures rise, offsets will become more negative because the parameter estimate for T_{macro} represents the proportional buffering of canopies of free-air temperatures. Offsets for T_{mean} and T_{min} were negatively affected by precipitation. That is, the buffering for T_{max} by canopies was stronger in regions with higher amounts of precipitation, whereas buffering is lower for T_{min}, supporting the notion that evapotranspiration drives the offset in these conditions (Davis et al., 2019). The limited role of drivers other than macroclimate could be because the 30 arcsec (~1 km) spatial resolution is still too coarse to detect effects of e.g. topography or canopy cover, drivers acting on a very local scale (Ashcroft & Gollan, 2012; Greiser et al., 2018; Macek et al., 2019).

Our aim was not to produce maps for use, but to give an overview of how temperature offsets between forest and open habitats vary across forest biomes and how these relationships can evolve under climate change. Despite the limitations of the data and the assumptions made, we found that our models explained a moderately large amount of variation in the offsets, and considered model accuracy to be fair. Uncertainty

in predictions increased towards tropical and boreal forests which is likely caused by extrapolation outside the environmental range included in our data. These biomes were underrepresented in the data, hence, future research should focus on setting out networks of paired temperature sensors in these regions (Lembrechts, Lenoir, Frenne, & Scheffers, 2021).

Our projections for both the "very stringent" RCP2.6 as well as the "worst-case" RCP8.5 scenario indicate that buffering by forest canopies for T_{mean} and T_{max} temperature may increase, but minimum temperature offsets will decrease, especially in temperate and boreal regions as ambient temperatures become less cold. This suggests that under climate change, free-air temperatures are likely to have a larger-magnitude increase than the corresponding forest microclimate temperatures, which would reinforce the idea of divergent warming (decoupling) between macroclimate and microclimate (De Frenne et al., 2019; Lenoir et al., 2017). Offsets may even become lower (resulting in increasing or decreasing buffering for T_{mean} or T_{min}, respectively) despite projected decreases in precipitation in some regions (Supplementary Fig. 9). It is possible that finer-grained microclimatic heterogeneity could buffer the impact of a changing macroclimate even further (Maclean, Suggitt, Wilson, Duffy, & Bennie, 2017). This inference relies, however, on the strong assumption that forest cover and composition will remain stable in the future. Such stability is however unlikely, as both climate change itself as forest management and disturbances can either increase or decrease forest canopy cover in the future. For example, climate change is however likely to cause increased tree mortality owing to, for instance, repeated and more severe disturbances such as droughts, fires, pathogens and insect outbreaks (Curtis, Slay, Harris, Tyukavina, & Hansen, 2018; Senf, Sebald, & Seidl, 2021; Senf & Seidl, 2020). The resulting reduction in tree canopy cover can lead to a sudden loss (i.e. a tipping point) of canopy buffering and increased microclimate warming (Alkama & Cescatti, 2016; Findell et al., 2017; Lembrechts & Nijs, 2020; Richard et al., 2021; Zellweger, De Frenne, Lenoir, Vangansbeke, Verheyen, Bernhardt-römermann, et al., 2020). On the other hand, strong efforts are being made worldwide to increase forest cover and implement climate-smart forestry practices (Bastin et al., 2019; Di Sacco et al., 2021). How these forest cover changes will affect future forest temperature buffering should be a topic for future forest microclimate research.

We projected temperature buffering capacities of forests across the globe under future climate change scenarios. Assuming no change in forest composition, we predicted that forests' buffering of T_{mean} and T_{max}

will increase in the future (2060-2080), whereas buffering of T_{min} will be reduced due to changes in macroclimate conditions. Our results indicate that the refugial capacity of cool and dense forest might last longer than anticipated in a warming climate. This knowledge has important implications for forest biodiversity conservation. Forest managers and policymakers could, for example, aim to optimise forest functioning and biodiversity goals by identifying areas in which reducing or retaining canopy cover may have larger impacts on the prevailing microclimate than anticipated under future climate change (Wolf et al., 2021). The paired nature of the data allowed us to model absolute temperature offsets across a global extent with fair accuracy. Gridded microclimate products such as ours, especially when paired with new, well-designed networks of microclimate measurements (Lembrechts et al., 2020) serve ecological and environmental modelers with a more scale-relevant set of products for making predictions and drawing inference. At the regional and even continental scale, novel high-resolution data on forest structure and composition based on remote sensing imagery (e.g. GEDI LiDAR data) are becoming available (De Frenne et al., 2021; Lembrechts et al., 2019; Randin et al., 2020; Zellweger, De Frenne, Lenoir, Rocchini, & Coomes, 2018). Including these microclimate measurements and novel spatial map data (e.g. Haesen et al., under review; Lembrechts et al., 2020) in future models and mapping efforts will increase accuracy of future predictions (Lembrechts, Hoogen, et al., 2021). Our study illustrates that forest microclimates themselves are subject to climate change, which will have important consequences for forest-dwelling species and must hence not be neglected.

Data availability:

The dataset analysed in the current study is available in the figshare repository, with the identifier 10.6084/m9.figshare.7604849 (de Frenne, Lenoir, & Rodriguez-Sanchez, 2019).

References

Alavi, S. J., Ahmadi, K., Hosseini, S. M., Tabari, M., & Nouri, Z. (2019). The response of English yew (Taxus baccata L.) to climate change in the Caspian Hyrcanian Mixed Forest ecoregion. *Regional Environmental Change*, *19*(5), 1495–1506. doi: 10.1007/s10113-019-01483-x

Alkama, R., & Cescatti, A. (2016). Climate change: Biophysical climate impacts of recent changes in global forest cover. *Science*, *351*(6273), 600–604. doi: 10.1126/science.aac8083

Amatulli, G., Domisch, S., Tuanmu, M. N., Parmentier, B., Ranipeta, A., Malczyk, J., & Jetz, W. (2018). Data Descriptor: A suite of global, cross-scale topographic variables for environmental and biodiversity modeling. *Scientific Data*, *5*, 1–15. doi: 10.1038/sdata.2018.40

Ashcroft, M. B., & Gollan, J. R. (2012). Fine-resolution (25 m) topoclimatic grids of near-surface (5 cm) extreme temperatures and humidities across various habitats in a large (200 × 300 km) and diverse region. *International Journal of Climatology*, *32*(14), 2134–2148. doi: 10.1002/joc.2428

Barton, K. (2009). *MuMIn: Multi-Model Inference*.

Bastin, J., Finegold, Y., Garcia, C., Mollicone, D., Rezende, M., Routh, D., … Crowther, T. (2019). The global tree restoration potential. *Science*, *365*, 76–79. doi: 10.1126/science.aay8060

Bates, D., Maechler, M., Bolker, B. M., & Walker, S. (2015). Fitting Linear Mixed-Effects Models Using lme4. *Journal Of Statistical Software*, *67*(1), 1–48. doi: 10.18637/jss.v067.i01

Chen, J., Saunders, S. C., Crow, T. R., Naiman, R. J., Brosofske, K. D., Mroz, G. D., … Franklin, J. F. (1999). Microclimate in forest ecosystem and landscape ecology: Variations in local climate can be used to monitor and compare the effects of different management regimes. *BioScience*, *49*(4), 288–297. doi: 10.2307/1313612

Chen, Y., Liu, Y., Zhang, J., Yang, W., He, R., & Deng, C. (2018). Microclimate exerts greater control over litter decomposition and enzyme activity than litter quality in an alpine forest-tundra ecotone. *Scientific Reports*, *8*(1), 1–13. doi: 10.1038/s41598-018-33186-4

Curtis, P. G., Slay, C. M., Harris, N. L., Tyukavina, A., & Hansen, M. C. (2018). Classifying drivers of global forest loss. *Science*, *361*(6407), 1108–1111. doi: 10.1126/science.aau3445

Davis, K. T., Dobrowski, S. Z., Holden, Z. A., Higuera, P. E., & Abatzoglou, J. T. (2019). Microclimatic buffering in forests of the future: the role of local water balance. *Ecography*, *42*(1), 1–11. doi: 10.1111/ecog.03836

De Frenne, P., Lenoir, J., Luoto, M., Scheffers, B. R., Zellweger, F., Aalto, J., … Hylander, K. (2021). Forest microclimates and climate change : Importance, drivers and future research agenda. *Global Change Biology*, (February), 1–19. doi: 10.1111/gcb.15569

de Frenne, P., Lenoir, J., & Rodriguez-Sanchez, F. (2019). Global buffering of temperatures under forest canopies data and code. *Figshare*. doi: 10.6084/m9.figshare.7604849

De Frenne, P., Rodríguez-Sánchez, F., Coomes, D. A., Baeten, L., Verstraeten, G., Vellend, M., … Verheyen, K. (2013). Microclimate moderates plant responses to macroclimate warming. *Proceedings of the National Academy of Sciences of the United States of America*, *110*(46), 18561–18565. doi: 10.1073/pnas.1311190110

De Frenne, P., Zellweger, F., Rodríguez-Sánchez, F., Scheffers, B. R., Hylander, K., Luoto, M., … Lenoir, J. (2019). Global buffering of temperatures under forest canopies. *Nature Ecology and Evolution*, *3*(5), 744–749. doi: 10.1038/s41559-019-0842-1

De Smedt, P., Boeraeve, P., & Baeten, L. (2021). Intra-annual activity patterns of terrestrial isopods are tempered in forest compared to open habitat. *Soil Biology and Biochemistry*, *160*(September 2020),

108342. doi: 10.1016/j.soilbio.2021.108342

Di Sacco, A., Hardwick, K. A., Blakesley, D., Brancalion, P. H. S., Breman, E., Cecilio Rebola, L., … Antonelli, A. (2021). Ten golden rules for reforestation to optimize carbon sequestration, biodiversity recovery and livelihood benefits. *Global Change Biology*, *27*(7), 1328–1348. doi: 10.1111/gcb.15498

Dietz, L., Collet, C., Dupouey, J. L., Lacombe, E., Laurent, L., & Gégout, J. C. (2020). Windstorm-induced canopy openings accelerate temperate forest adaptation to global warming. *Global Ecology and Biogeography*, (March), 2067–2077. doi: 10.1111/geb.13177

Fick, S. E., & Hijmans, R. J. (2017). WorldClim 2: new 1-km spatial resolution climate surfaces for global land areas. *International Journal of Climatology*, *37*(12), 4302–4315. doi: 10.1002/joc.5086

Findell, K. L., Berg, A., Gentine, P., Krasting, J. P., Lintner, B. R., Malyshev, S., … Shevliakova, E. (2017). The impact of anthropogenic land use and land cover change on regional climate extremes. *Nature Communications*, *8*(1), 1–9. doi: 10.1038/s41467-017-01038-w

Frey, S. J. K., Hadley, A. S., & Betts, M. G. (2016). Microclimate predicts within-season distribution dynamics of montane forest birds. *Diversity and Distributions*, *22*(9), 944–959. doi: 10.1111/ddi.12456

Frey, S. J. K., Hadley, A. S., Johnson, S. L., Schulze, M., Jones, J. A., & Betts, M. G. (2016). Spatial models reveal the microclimatic buffering capacity of old-growth forests. *Science Advances*, *2*(4). doi: 10.1126/sciadv.1501392

Geiger, R., Aron, R., & Todhunter, P. (2009). *The climate near the ground*. Rowman & Littlefield.

Greiser, C., Meineri, E., Luoto, M., Ehrlén, J., & Hylander, K. (2018). Monthly microclimate models in a managed boreal forest landscape. *Agricultural and Forest Meteorology*, *250–251*(December 2017), 147–158. doi: 10.1016/j.agrformet.2017.12.252

Hansen, M. C., Potapov, P. V, Moore, R., Hancher, M., Turubanova, S. A., Tyukavina, A., … Townshend, J. R. G. (2013). High-Resolution Global Maps of 21st-Century Forest Cover Change. *Science*, *342*, 850–854. doi: 10.1126/science.1244693

Hijmans, R. J., & van Etten, J. (2012). *raster: Geographic analysis and modeling with raster data*.

IPCC. (2018). Global Warming of 1.5 °C - SR15 - Summary for Policy Makers. In *IPCC Climate Change Synthesis Report*.

Lembrechts, J. J., Aalto, J., Ashcroft, M. B., De Frenne, P., Kopecký, M., Lenoir, J., … Nijs, I. (2020). SoilTemp: A global database of near-surface temperature. *Global Change Biology*, *26*(11), 6616–6629. doi: 10.1111/gcb.15123

Lembrechts, J. J., Hoogen, J. Van Den, Aalto, J., Ashcroft, M. B., De Frenne, P., Kemppinen, J., & Kopecký, M. (2021). Mismatches between soil and air temperature. *EcoEvoRxiv*. doi: 10.32942/osf.io/pksqw

Lembrechts, J. J., Lenoir, J., Frenne, P. De, & Scheffers, B. R. (2021). *Designing countrywide and regional microclimate networks*. (February), 1–7. doi: 10.1111/geb.13290

Lembrechts, J. J., & Nijs, I. (2020). Microclimate shifts in a d ynamic world. *Science*, *368*(6492), 711–712.

Lembrechts, J. J., Nijs, I., & Lenoir, J. (2019). Incorporating microclimate into species distribution models. *Ecography*, *42*(7), 1267–1279. doi: 10.1111/ecog.03947

Lenoir, J., Hattab, T., & Pierre, G. (2017). Climatic microrefugia under anthropogenic climate change: implications for species redistribution. *Ecography*, *40*(2), 253–266. doi: 10.1111/ecog.02788

Li, Y., Zhao, M., Motesharrei, S., Mu, Q., Kalnay, E., & Li, S. (2015). Local cooling and warming effects of forests based on satellite observations. *Nature Communications*, *6*. doi: 10.1038/ncomms7603

Macek, M., Kopecký, M., & Wild, J. (2019). Maximum air temperature controlled by landscape topography

affects plant species composition in temperate forests. *Landscape Ecology*, *34*(11), 2541–2556. doi: 10.1007/s10980-019-00903-x

Maclean, I. M. D., Suggitt, A. J., Wilson, R. J., Duffy, J. P., & Bennie, J. J. (2017). Fine-scale climate change: modelling spatial variation in biologically meaningful rates of warming. *Global Change Biology*, *23*(1), 256–268. doi: 10.1111/gcb.13343

Nakagawa, S., & Schielzeth, H. (2013). A general and simple method for obtaining R2 from generalized linear mixed-effects models. *Methods in Ecology and Evolution*, *4*(2), 133–142. doi: 10.1111/j.2041-210x.2012.00261.x

Olson, D. M., Dinerstein, E., Wikramanayake, E. D., Burgess, N. D., Powell, G. V. N., Underwood, E. C., … Kassem, K. R. (2001). *Terrestrial Ecoregions of the World : A New Map of Life on Earth*. *51*(11), 933–938.

Paradis, E., & Schliep, K. (2019). Ape 5.0: An environment for modern phylogenetics and evolutionary analyses in R. *Bioinformatics*, *35*(3), 526–528. doi: 10.1093/bioinformatics/bty633

R Core Team. (2021). *R: A language and environment for statistical computing*.

Randin, C. F., Ashcroft, M. B., Bolliger, J., Cavender-Bares, J., Coops, N. C., Dullinger, S., … Payne, D. (2020). Monitoring biodiversity in the Anthropocene using remote sensing in species distribution models. *Remote Sensing of Environment*, *239*(January), 111626. doi: 10.1016/j.rse.2019.111626

Richard, B., Dupouey, J. L., Corcket, E., Alard, D., Archaux, F., Aubert, M., … Lenoir, J. (2021). The climatic debt is growing in the understorey of temperate forests: Stand characteristics matter. *Global Ecology and Biogeography*, *30*(7), 1474–1487. doi: 10.1111/geb.13312

Sanderson, B. M., Knutti, R., & Caldwell, P. (2015). A representative democracy to reduce interdependency in a multimodel ensemble. *Journal of Climate*, *28*(13), 5171–5194. doi: 10.1175/JCLI-D-14-00362.1

Senf, C., Sebald, J., & Seidl, R. (2021). Increasing canopy mortality affects the future demographic structure of Europe's forests. *One Earth*, 1–7. doi: 10.1016/j.oneear.2021.04.008

Senf, C., & Seidl, R. (2020). Mapping the forest disturbance regimes of Europe. *Nature Sustainability*. doi: 10.1038/s41893-020-00609-y

Simard, M., Pinto, N., Fisher, J. B., & Baccini, A. (2011). Mapping forest canopy height globally with spaceborne lidar. *Journal of Geophysical Research: Biogeosciences*, *116*(4), 1–12. doi: 10.1029/2011JG001708

Stevens, J. T., Safford, H. D., Harrison, S., & Latimer, A. M. (2015). Forest disturbance accelerates thermophilization of understory plant communities. *Journal of Ecology*, *103*(5), 1253–1263. doi: 10.1111/1365-2745.12426

Tennekes, M. (2018). Tmap: Thematic maps in R. *Journal of Statistical Software*, *84*(6). doi: 10.18637/jss.v084.i06

Thrippleton, T., Bugmann, H., Kramer-Priewasser, K., & Snell, R. S. (2016). Herbaceous Understorey : An Overlooked Player in Forest Landscape Dynamics? *Ecosystems*, *19*(7), 1240–1254. doi: 10.1007/s10021-016-9999-5

Von Arx, G., Graf Pannatier, E., Thimonier, A., & Rebetez, M. (2013). Microclimate in forests with varying leaf area index and soil moisture: Potential implications for seedling establishment in a changing climate. *Journal of Ecology*, *101*(5), 1201–1213. doi: 10.1111/1365-2745.12121

Wickham, H. (2016). *ggplot2: elegant graphics for data analysis*. New York, USA: Springer.

Wolf, C., Bell, D. M., Kim, H., Paul, M., Schulze, M., Betts, M. G., … Or, C. (2021). Temporal consistency of undercanopy thermal refugia in old-growth forest. *Agricultural and Forest Meteorology*, *307*(April), 108520. doi: 10.1016/j.agrformet.2021.108520

Wood, S., & Scheipl, F. (2014). *gamm4: Generalized additive mixed models using mgcv and lme4*.

World Meteorological Organization. (2018). *Guide to meteorological instruments and methods of observation* (2018 Editi). WMO.

Zellweger, F., Coomes, D., Lenoir, J., Depauw, L., Maes, S. L., Wulf, M., … De Frenne, P. (2019). Seasonal drivers of understorey temperature buffering in temperate deciduous forests across Europe. *Global Ecology and Biogeography*, *28*(12), 1774–1786. doi: 10.1111/geb.12991

Zellweger, F., De Frenne, P., Lenoir, J., Rocchini, D., & Coomes, D. (2018). Advances in microclimate ecology arising from remote sensing. *Trends in Ecology & Evolution*, *xx*, 1–15. doi: 10.1016/j.tree.2018.12.012

Zellweger, F., De Frenne, P., Lenoir, J., Vangansbeke, P., Verheyen, K., Bernhardt-römermann, M., … Chudomelov. (2020). Forest microclimate dynamics drive plant responses to warming. *Science*, *368*(May), 772–775.

Zellweger, F., De Frenne, P., Lenoir, J., Vangansbeke, P., Verheyen, K., Bernhardt-Römermann, M., … Coomes, D. (2020). Forest microclimate dynamics drive plant responses to warming. *Science*, *in press*.

Zuur, A. F., Ieno, E. N., & Elphick, C. S. (2010). *A protocol for data exploration to avoid common statistical problems*. 3–14. doi: 10.1111/j.2041-210X.2009.00001.x

Supporting information

Appendix S1: Supplementary analysis for variation between seasons

Due to the low number of observations for each season for all three temperature responses (Table S1.1), we have not included this analysis in the main text.

Table S1.1. Number of observations for each response variable for the three seasonal categories.

	Annual	Growing season	Non-growing season
T_{mean}	10	196	63
T_{max}	11	118	46
T_{min}	11	141	37

Only for T_{mean} offsets do we show predictions as we found that only for this response the categorical variable for season was included in best model.

Table S1.2.

	Mean temperature offset			**Max. temperature offset**			**Min. temperature offset**		
Predictors	*Estimates*	*CI*	*p*	*Estimates*	*CI*	*p*	*Estimates*	*CI*	*p*
(Intercept)	-1.97	-3.28 – -0.66	**0.003**	-2.97	-3.90 – -2.04	**<0.001**	1.38	0.97 – 1.79	**<0.001**
Height.sensor	0.37	0.17 – 0.56	**<0.001**	1.98	1.37 – 2.60	**<0.001**	-0.43	-0.70 – -0.16	**0.002**
Prec	-0.47	-0.97 – 0.04	0.072	-1.24	-2.13 – -0.35	**0.006**	-0.69	-1.21 – -0.17	**0.010**
Tmacro	-0.76	-1.24 – -0.29	**0.002**				-0.33	-0.73 – 0.07	0.105
Season_num [2]	1.84	0.53 – 3.14	**0.006**						
Season_num [3]	0.61	-0.66 – 1.88	0.346						
TPI				0.72	0.05 – 1.39	**0.036**			
Dist2coast2							-0.33	-0.72 – 0.05	0.086
Forest_cover							0.50	0.06 – 0.95	**0.027**
Northness							0.34	0.04 – 0.64	**0.024**
Random Effects									
σ^2	1.75			8.20			1.42		
τ_{00}	2.32 $_{Study.ID}$			5.18 $_{Study.ID}$			1.01 $_{Study.ID}$		
ICC	0.57			0.39			0.42		
N	41 $_{Study.ID}$			39 $_{Study.ID}$			38 $_{Study.ID}$		
Observations	269			175			189		
Marginal R^2 / Conditional R^2	0.253 / 0.679			0.268 / 0.552			0.253 / 0.564		

We found that the offsets during the growing season are lower than offsets during the non-growing season. The annual measurements were expected to be the average of offsets from growing and non-growing seasons. This was however not the case and is likely due to the low number of annual measurements.

(A) Tmean offset for annual measurements (1970-2000)

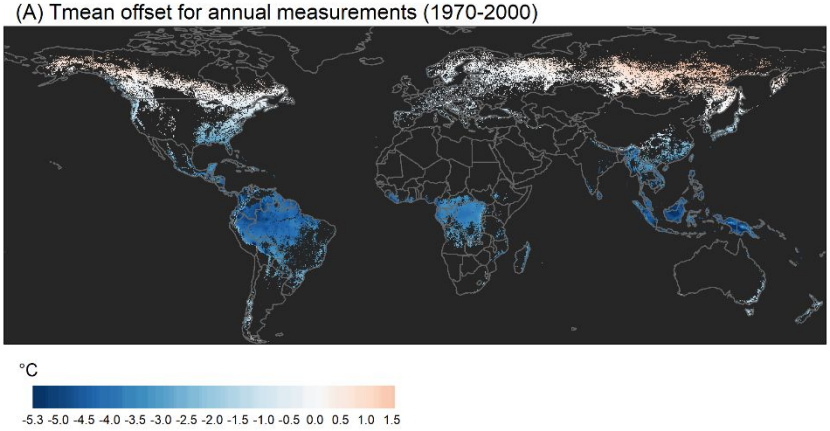

(B) Tmean offset for non-growing season (1970-2000)

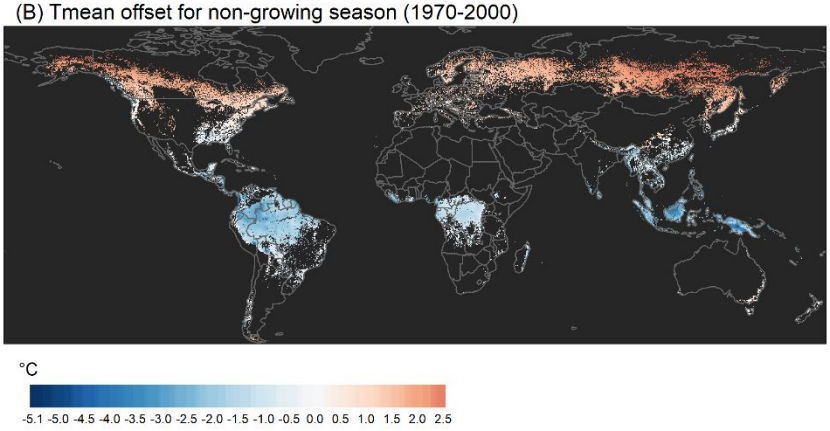

(C) Tmean offset for growing season (1970-2000)

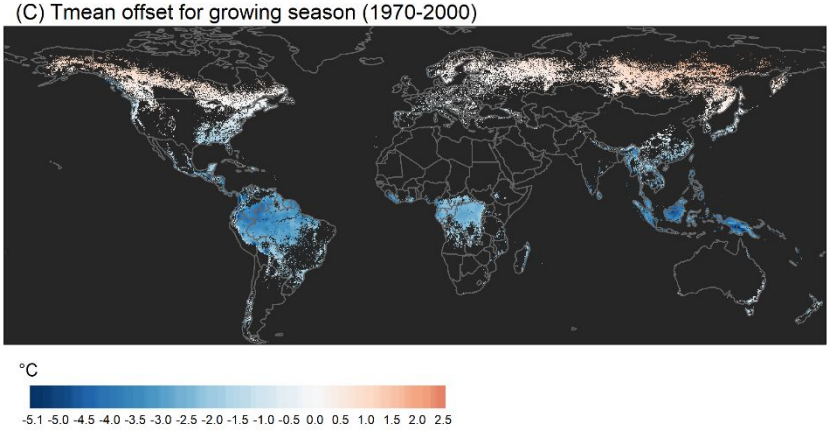

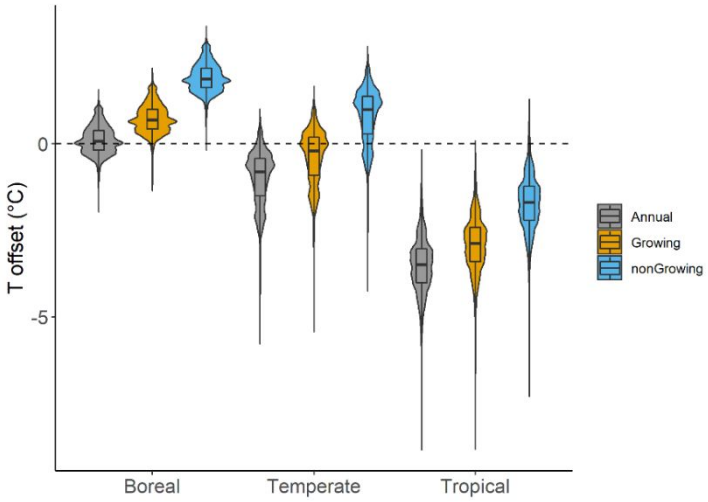

Fig S1.1. Global predictions for T_{mean} offsets including season of sampling (A: annual measurements [n=10], B: growing seasons [n=196], C: non-growing season [n=63]) in the single best model. Panel (D): violin and box plots showing the distribution for the offsets of (A), (B) and (C) across boreal, temperate and tropical forests classified following Olson et al. (2012). For T_{max} and T_{min} offsets, season did not have a significant effect and are thus not shown.

Appendix S2: Supporting figures and tables

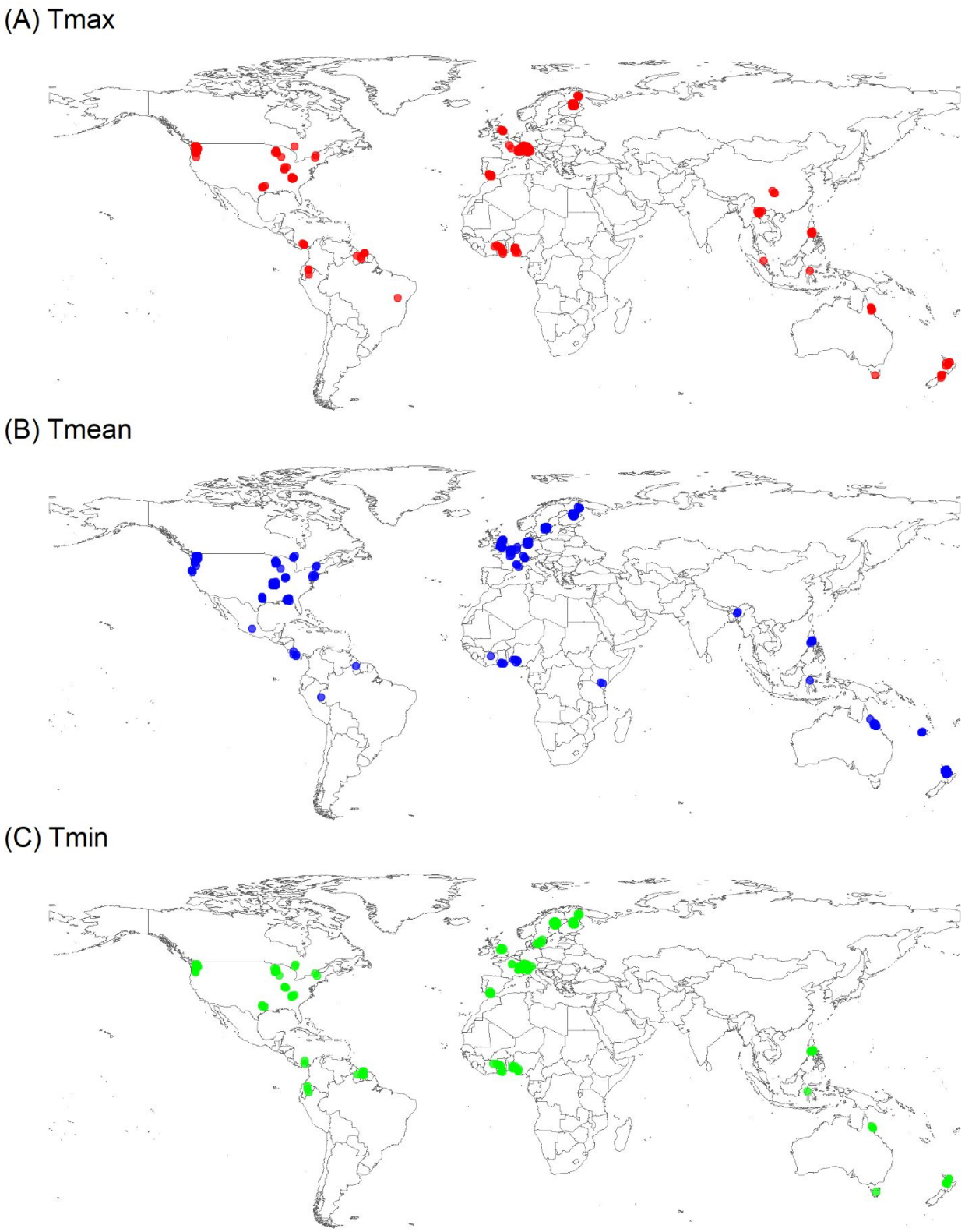

Supplementary Fig. 1. Distribution of the data points used in this study for (A) T_{max}, (B) T_{mean} and (C) T_{min}.

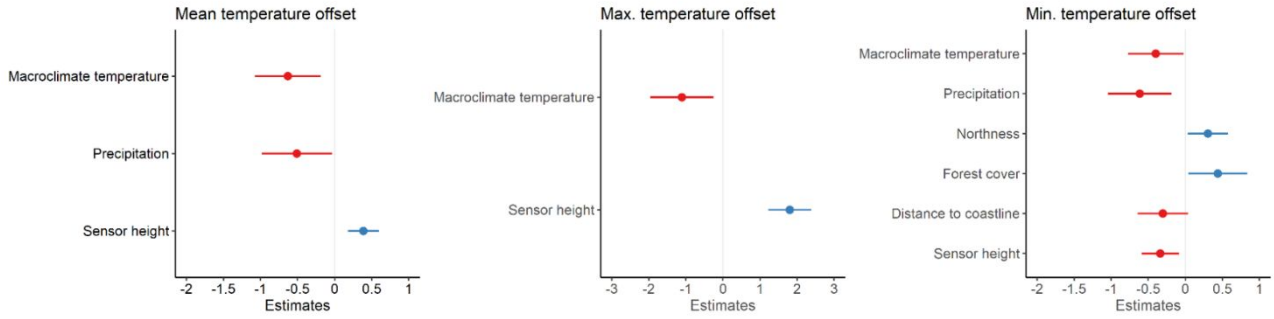

Supplementary Fig. 2. Parameter estimates and 95% confidence intervals for the variables that were retained in the single best models for each of the three responses.

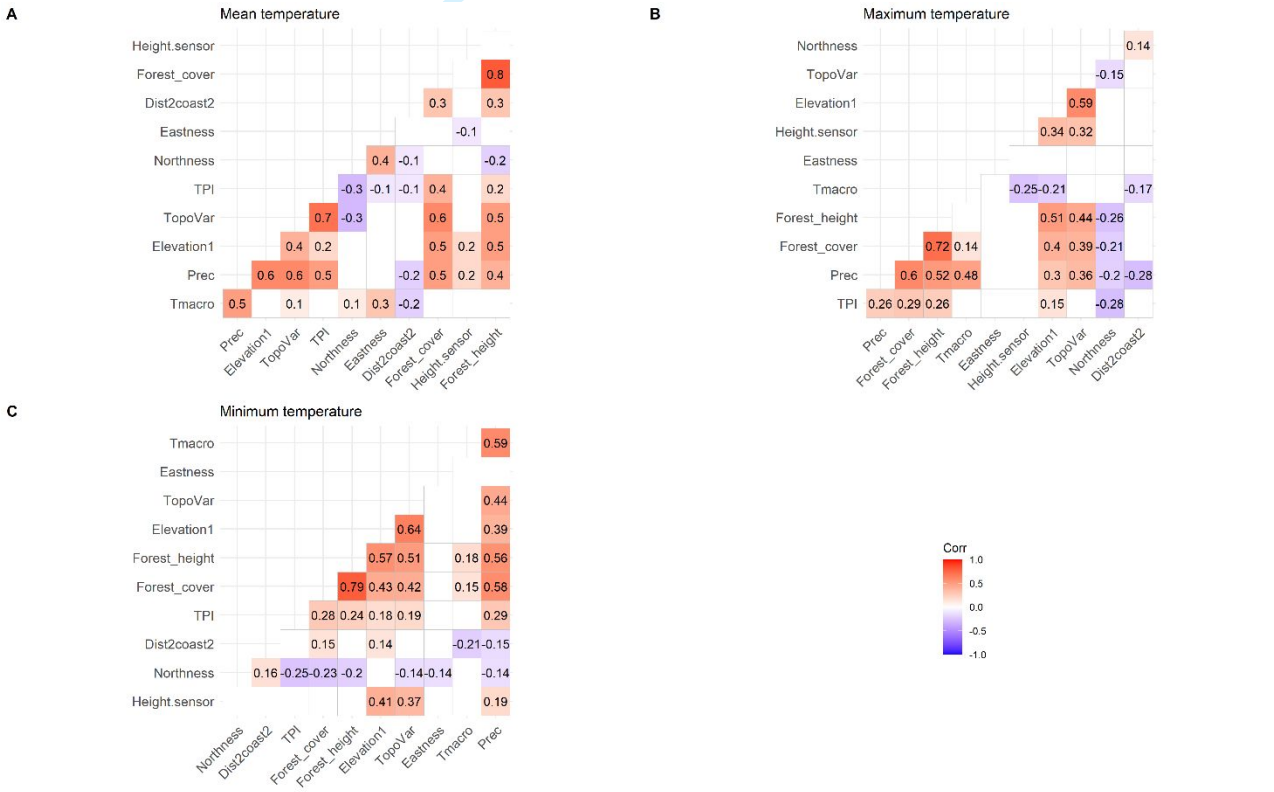

Supplementary Fig. 3. Correlograms of the used predictor variables.

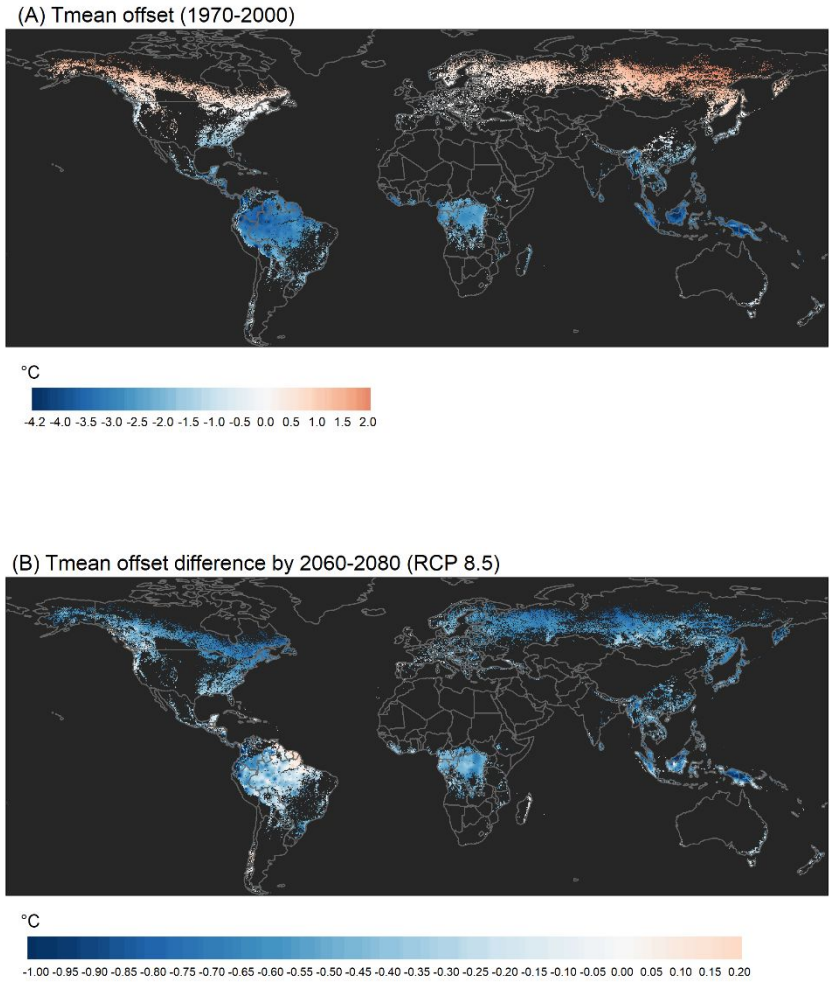

Supplementary Fig. 4. (A) Global map of past (1970-2000 climate) forest temperature offsets of mean temperatures below tree canopies. (B) Map showing the difference between mean offset predictions based on future climatic conditions under RCP8.5 scenarios and past (1970-2000) offsets (future minus past, negative values thus depict more negative future than past offsets). Predictions were made based on linear mixed-effects models only for pixels where the canopy cover in the year 2000 is > 50% (Hansen et al., 2013).

Supplementary Table. 1. Statistical relationships between temperature offsets (i.e. the response variable) and predictor variables retained in the single best models for mean (T_{mean}), maximum (T_{max}) and minimum (T_{min}) temperatures, separately. Results from mixed-effect models taking the non-independence of data from the same study into account by including a random-effect term 'study'.

(A)

	Mean temperature offset			**Max. temperature offset**			**Min. temperature offset**		
Predictors	*Estimates*	*CI*	*p*	*Estimates*	*CI*	*p*	*Estimates*	*CI*	*p*
(Intercept)	-1.15	-1.66 – -0.64	**<0.001**	-3.16	-4.08 – -2.23	**<0.001**	1.28	0.92 – 1.65	**<0.001**
Height.sensor	0.39	0.18 – 0.60	**<0.001**	1.80	1.23 – 2.38	**<0.001**	-0.34	-0.59 – -0.09	**0.009**
Prec	-0.51	-0.98 – -0.04	**0.035**				-0.61	-1.04 – -0.19	**0.005**
Tmacro	-0.63	-1.08 – -0.19	**0.005**	-1.11	-1.96 – -0.25	**0.011**	-0.40	-0.77 – -0.02	**0.037**
Dist2coast2							-0.30	-0.64 – 0.04	0.081
Forest_cover							0.44	0.04 – 0.84	**0.030**
Northness							0.31	0.03 – 0.58	**0.028**
Random Effects									
σ^2	1.98			7.99			1.43		
τ_{00}	1.88 $_{Study.ID}$			5.47 $_{Study.ID}$			0.81 $_{Study.ID}$		
ICC	0.49			0.41			0.36		
N	43 $_{Study.ID}$			43 $_{Study.ID}$			42 $_{Study.ID}$		
Observations	274			188			202		
Marginal R^2 / Conditional R^2	0.215 / 0.597			0.289 / 0.578			0.248 / 0.520		

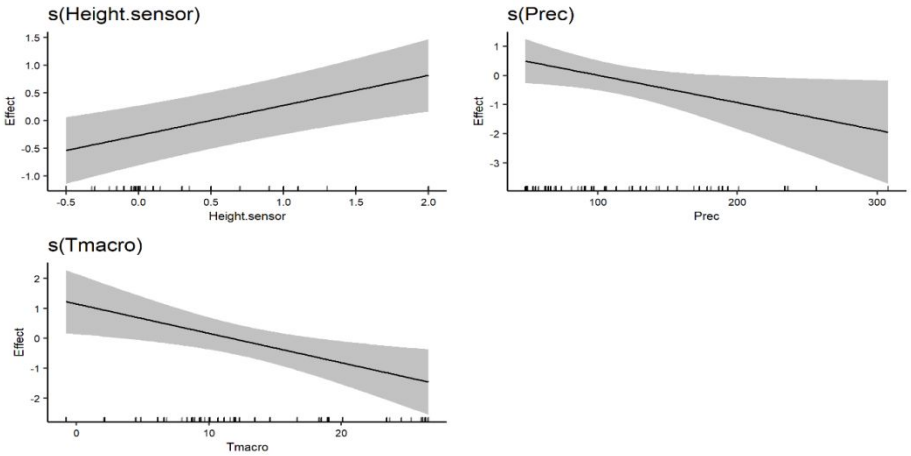

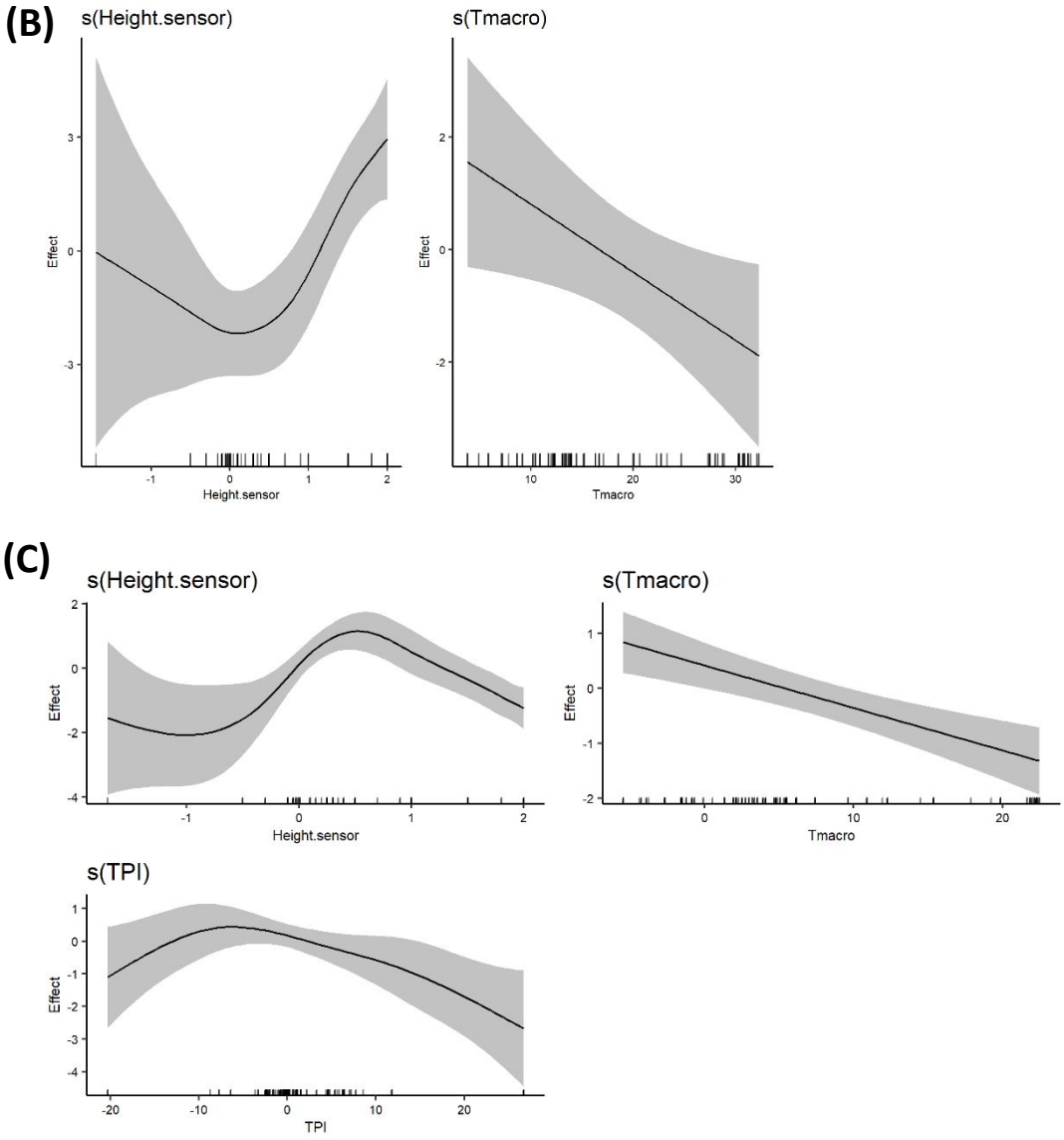

Supplementary Fig. 5. Estimated smooths with 95% credible intervals for the parameters that were retained in the single best GAMM models for (A) T_{mean}, (B) T_{max}, and (C) T_{min}, from top to bottom mean, maximum and minimum temperature offset. Dashes on the x-axis shows the distribution of raw data points.

Supplementary Table 2. Overview of global averages and 95% confidence intervals of the mean and standard deviations of the temperature offsets for the 30 bootstraps for past, and future climatic conditions.

		Mean (95% CI)	SD (95% CI)
T_{max}	past	-2.9 (-4.9, -0.5)	0.4 (0.2, 0.7)
	RCP2.6	-3.2 (-5.2, -0.8)	0.4 (0.2, 0.7)
	RCP8.5	-3.5 (-5.5, -1.1)	0.4 (0.2, 0.6)
T_{mean}	past	-0.9 (-4.1, 1.9)	0.3 (0.1, 0.5)
	RCP2.6	-1.1 (-4.4, 1.6)	0.4 (0.2, 0.8)
	RCP8.5	-1.4 (-4.7, 1.2)	0.5 (0.3, 0.7)
T_{min}	past	0.9 (-1.6, 3)	0.4 (0.2, 0.8)
	RCP2.6	0.7 (-1.7, 2.8)	0.5 (0.2, 0.9)
	RCP8.5	0.6 (-1.9, 2.6)	0.5 (0.2, 1)

Mean Tmax offsets Past	Standard deviation
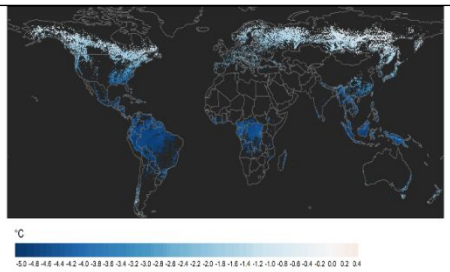	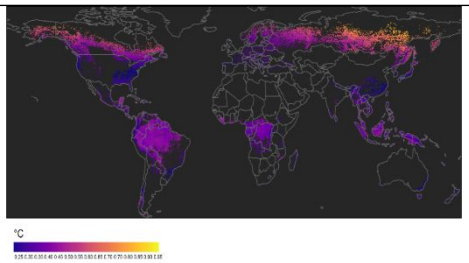
RCP2.6	
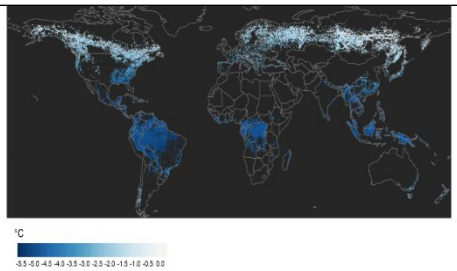	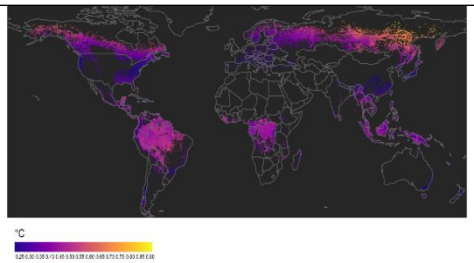
RCP8.5	
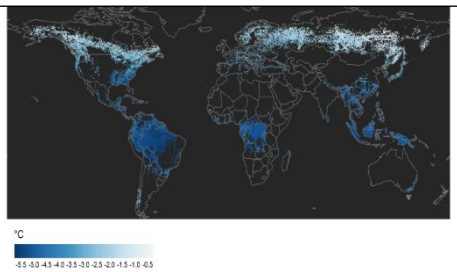	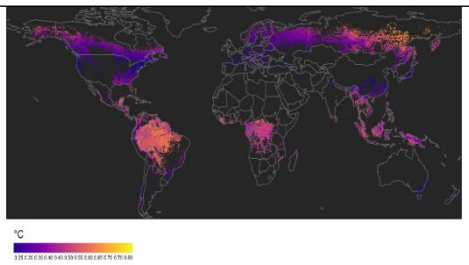

Mean Tmean offsets	Standard deviation
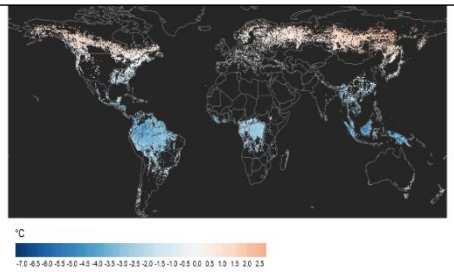	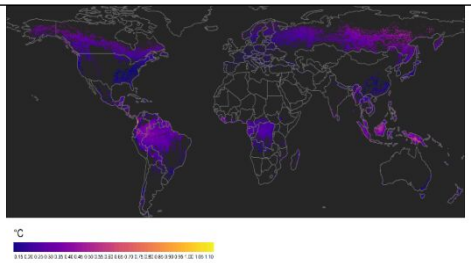

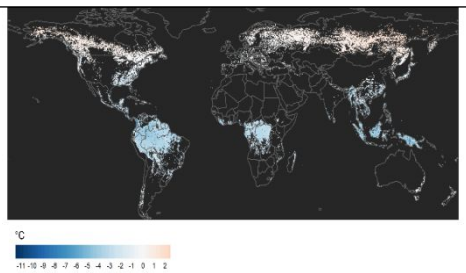

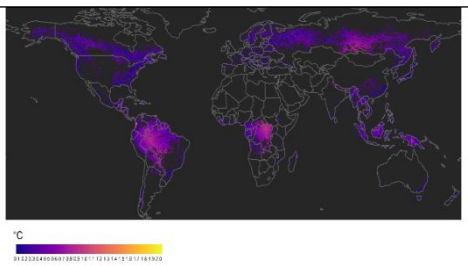

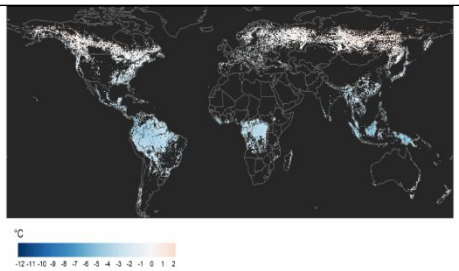

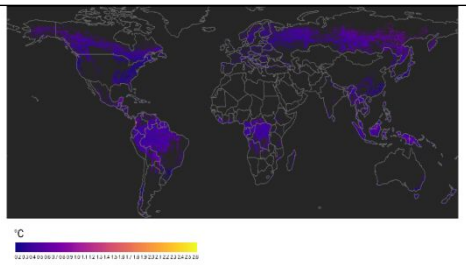

Mean Tmin offsets	Standard deviation

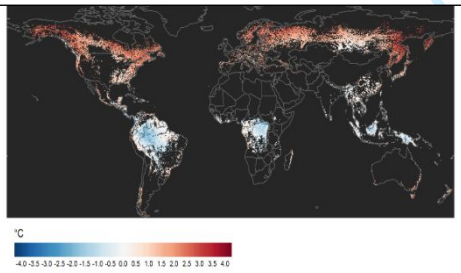

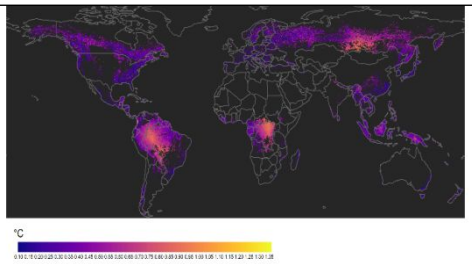

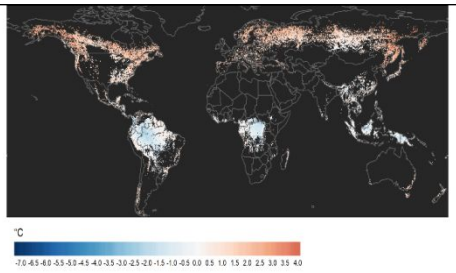

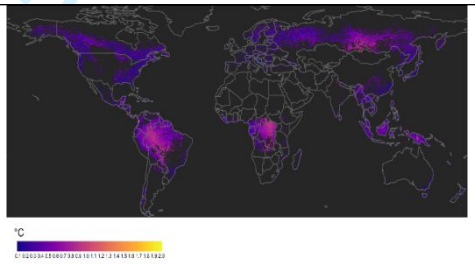

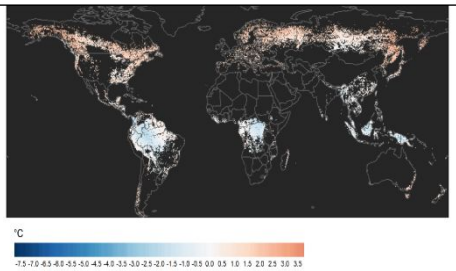

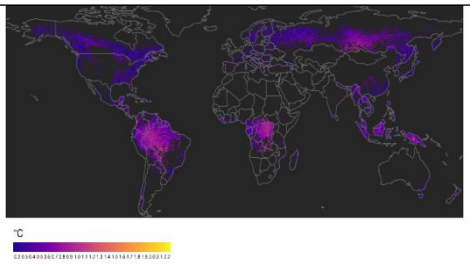

Supplementary Fig. 6. Global maps of the mean (left panels) and the standard deviation (right panels) for the 30 bootstrap samples (accounting for the fixed effects in the models). Maps are shown for past, future RCP2.6 and future RCP8.5 climatic conditions, for each of the three temperature responses. Predictions were made based on linear mixed-effects models only for pixels where the canopy cover in the year 2000 is > 50% (Hansen et al., 2013).

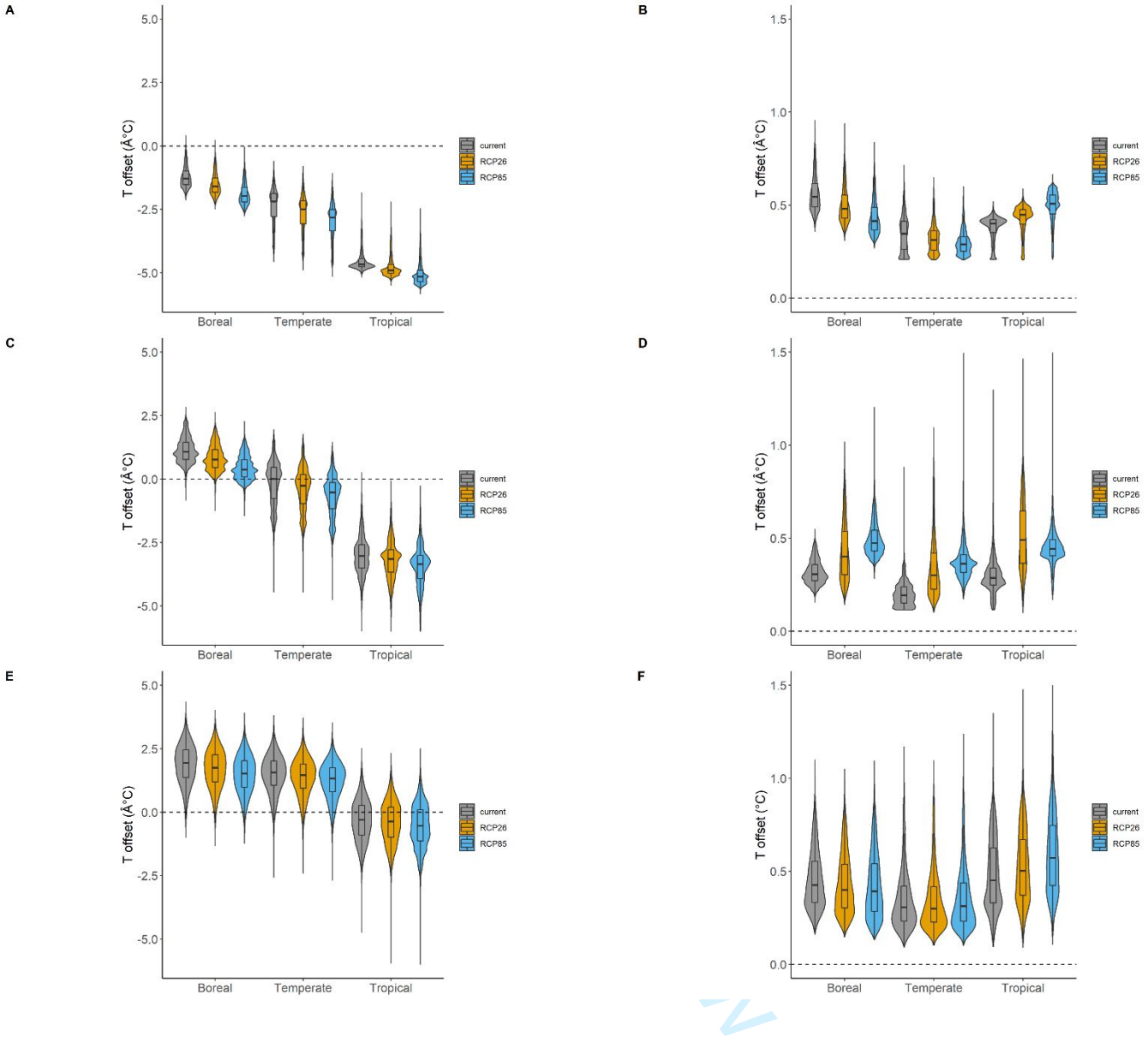

Supplementary Fig. 7. Violin and box plots of the mean (left panels) and standard deviation (right panels) of Tmax (panels A, B), Tmean (C, D) and Tmin (E, F) offsets for past and future (RCP2.6 and RCP8.5) climate conditions based on 30 bootstraps samples. Different colours and line types represent predictions for past climatic conditions (macroclimate temperature and precipitation, grey), for RCP2.6 (orange) and RCP2.8 scenarios (blue). Data points to draw these plots are subsamples (10^5 pixels) derived from the global predictions in Supplementary Fig. 7.

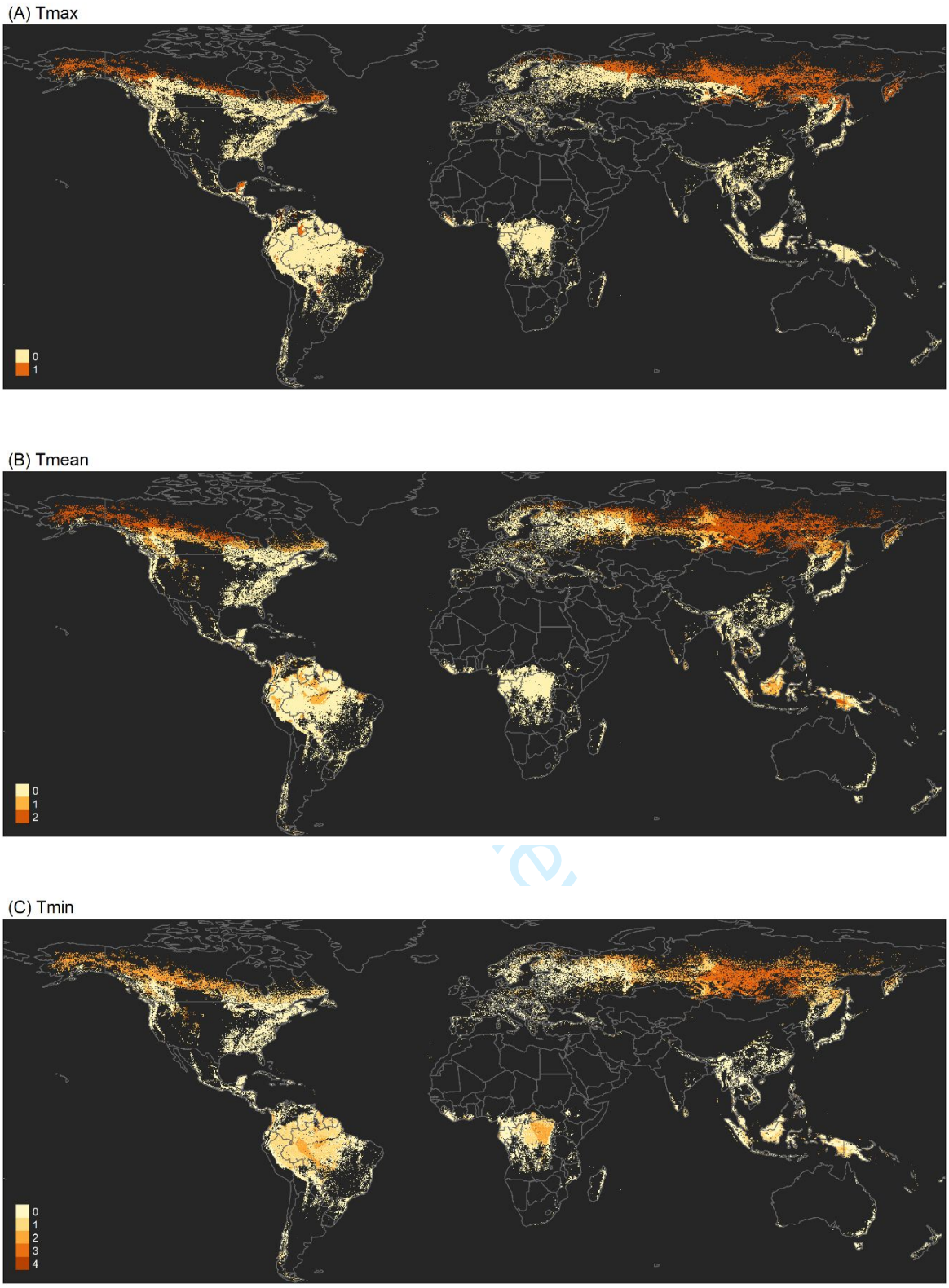

Supplementary Fig. 8. Maps showing extrapolation for (A) T_{max}, (B) T_{mean} and (C) T_{min}. Colors represent for each pixel for how many of the predictor variables the models extrapolate beyond the range used to calibrate the model.

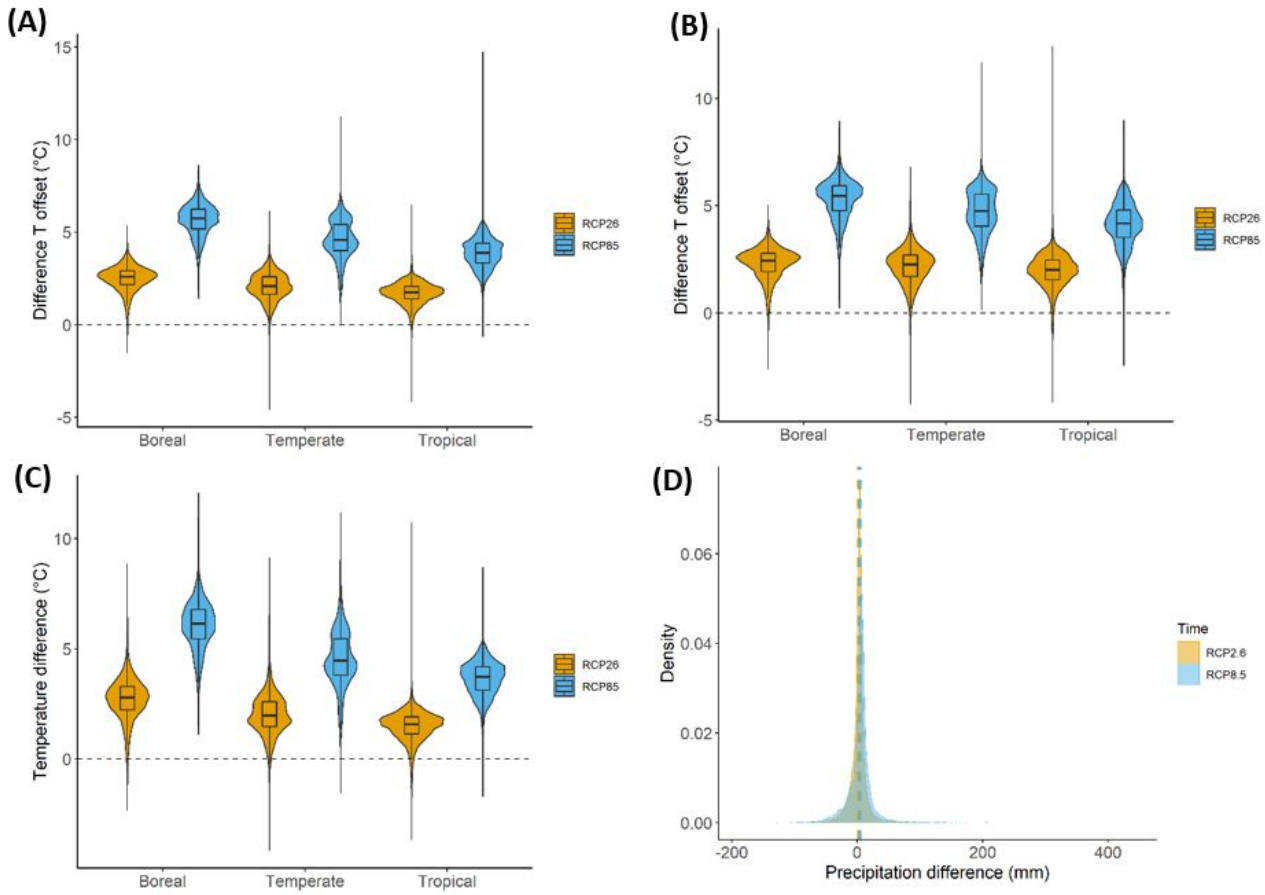

Supplementary Fig. 9. Violin plots and density plot of difference between past and future conditions (RCP2.6 and RCP8.5) for macroclimate temperature, (A) T_{mean}, (B) T_{max}, (C) T_{min}. for the pixels with canopy cover > 50%. (D) Shows the density plot for difference in precipitation between past and future. Data points to draw up these plots are subsamples derived from global maps of the WorldClim CMIP5 data using three GCMs (HadGEM2-ES, MPI-ESM-LR and MIROC5).